

Scattering of electrons by hydrogen atoms at intermediate energies: Elastic differential cross sections from 10 to 30 eV

Joseph Callaway*

Department of Mathematics, Imperial College, London SW 7 2RH, England

J. F. Williams

Department of Physics, The Queen's University, Belfast BT7 1NN, Northern Ireland

(Received 19 May 1975; revised manuscript received 11 August 1975)

The elastic scattering amplitude obtained from an open pseudostate calculation employing the algebraic variational method for partial waves of angular momentum $0 < L < 3$, is combined with phase shifts obtained in the extended polarization approximation for $4 < L < 99$ to obtain elastic differential cross sections for electron-hydrogen scattering for electron energies in the range 10–30 eV. Elastic angular distributions have been measured using a crossed-electron modulated-atom-beam method and absolute cross-section values determined using a phase-shift analysis method. The measurements include energies from 10 to 30 eV and angles from 10° to 140° with estimated experimental error limits of $\pm 17\%$. Within these error limits they are in agreement with the theoretical predictions except at 20 to 26 eV for angles greater than or equal to 120° , where the theoretical values are significantly higher than allowed by these error limits.

I. INTRODUCTION

This paper presents a joint theoretical and experimental study of the elastic differential cross sections for the scattering of electrons from atomic hydrogen over the energy region from 10–30 eV. Previous experimental studies¹ have measured absolute cross-section values, which are predicted within the experimental error limits of $\pm 6\%$ with 68% confidence and over the whole experimental energy range from 0.5–8.7 eV by those theoretical approximations which correctly allow for the effects of the long-range polarization potential. The only previous measurements in the energy region of 10–30 eV were the normalized relative angular distributions of Teubner *et al.*² at 12 and 20 eV, and those of Lloyd *et al.*³ at 30 eV. Our experimental study has measured absolute differential elastic cross sections at six of the incident-electron wave numbers k , equal to (in units of a_0^{-1} , the reciprocal of the Bohr radius) 0.94, 1.1, 1.2, 1.3, 1.4 and 1.5, that is, energies from 12–30 eV, at which our theoretical studies have been made. At these higher energies, excitation and continuum channel coupling effects as well as the need to consider more partial waves complicate the theoretical model.

The present theoretical approach is an extension of recent work^{4,5} in which a pseudostate expansion has been employed in combination with a variational method⁶ to obtain total cross sections for elastic scattering over the energy range 10–30 eV. The variational pseudostate calculation with the existing program becomes quite time consuming as the total angular momentum L increases. It

suffices to include contributions from states with $L < 3$ to obtain a good estimate (estimated error 2%) of the total elastic cross section; however, many more partial waves are required to obtain the correct differential cross section. This is a consequence of the relatively long-range polarization potential. In the present calculation, the scattering amplitude for states with $0 < L < 3$ has been taken from the pseudostate calculation, while for higher angular momentum ($4 < L < 99$) it has been determined approximately, according to the extended polarization method.⁷ This procedure will be discussed below.

II. THE PSEUDOSTATE CALCULATION

Since a detailed account of the pseudostate calculation has been published elsewhere,^{4,8} only a brief description will be given here. The hydrogen atom is represented by a set of eleven states, including the exact $1s$, $2s$, $2p$, and $3d$ states plus seven pseudostates, three of s type, three of p type, and one of d type. These states are orthogonal, and are a set of approximate eigenfunctions of the isolated hydrogen atom found by diagonalizing a matrix representing the Hamiltonian of the hydrogen atom on a basis of Slater-type orbitals. The parameters and energies of the pseudostate basis are given by Callaway and Wooten.⁴

This selection of states leads to a system of 19 coupled channels. The pseudochannels as well as the real ones are allowed to be open. This procedure was first employed by Burke and Webb.⁹ However, the use of open pseudostates may pro-

TABLE I. Comparison of elastic scattering amplitudes, $L=0$. CE refers to the complex energy extrapolation of McDonald and Nuttall.

k	$S=0$		$S=1$	
	Present	CE	Present	CE
1.1	$0.374 \pm 0.452i$	$0.37 \pm 0.47i$	$0.232 + 0.938i$	$0.232 \pm 0.938i$
1.2	$0.364 + 0.444i$	$0.35 + 0.45i$	$0.297 + 0.893i$	$0.298 + 0.893i$
1.3	$0.335 + 0.448i$	$0.34 + 0.43i$	$0.348 + 0.845i$	$0.350 + 0.845i$
1.4	$0.322 + 0.424i$	$0.33 + 0.42i$	$0.387 + 0.796i$	$0.386 + 0.795i$
1.5	$0.329 + 0.401i$	$0.33 + 0.41i$	$0.418 + 0.747i$	$0.422 + 0.749i$

duce unphysical structure in the cross sections associated with the thresholds of the open pseudo-channels.¹⁰ In order to avoid this problem, the parameters of the pseudostate basis are altered to move artificial thresholds away from energies at which calculations are desired.

The variational methods employed do not pro-

duce an exact solution of the coupled integro-differential equations; rather, variational estimates of certain quantities (in this case, the reactance matrix R) are obtained. These estimates are not bounds in the energy range of interest here. Additional complications are introduced by anomalies produced by singularities of certain

TABLE II. $1s-1s$ elastic scattering amplitude. R and I denote real and imaginary parts, respectively.

k^2	$L=0$		$L=1$		$L=2$		$L=3$	
	$S=0$	$S=1$	$S=0$	$S=1$	$S=0$	$S=1$	$S=0$	$S=1$
0.76 R	0.446	0.015	-0.007	0.378	0.080	0.078		
I	0.540	0.999	0.019	0.183	0.029	0.006		
0.78 R	0.436	0.028	0.000	0.378	0.088	0.080		
I	0.533	0.999	0.014	0.184	0.032	0.007		
0.81 R	0.425	0.047	0.006	0.378	0.092	0.082		
I	0.519	0.997	0.015	0.186	0.038	0.007		
0.83 R	0.422	0.059	0.009	0.377	0.093	0.084		
I	0.509	0.996	0.018	0.187	0.043	0.008		
0.85 R	0.427	0.071	0.011	0.377	0.090	0.085	0.036	0.036
I	0.497	0.994	0.021	0.186	0.049	0.008	0.002	0.004
0.90 R	0.419	0.099	0.007	0.377	0.089	0.088	0.039	0.038
I	0.500	0.989	0.032	0.187	0.052	0.010	0.004	0.005
0.95 R	0.402	0.125	0.018	0.377	0.091	0.092	0.041	0.039
I	0.483	0.983	0.029	0.189	0.059	0.011	0.006	0.007
1.00 R	0.426	0.148	0.021	0.377	0.078	0.095	0.044	0.040
I	0.461	0.975	0.036	0.186	0.071	0.012	0.007	0.008
1.10 R	0.383	0.191	0.030	0.376	0.087	0.099	0.048	0.043
I	0.468	0.959	0.042	0.188	0.071	0.015	0.011	0.011
1.21 R	0.374	0.232	0.033	0.372	0.075	0.104	0.050	0.044
I	0.452	0.938	0.053	0.185	0.080	0.017	0.017	0.012
1.44 R	0.364	0.297	0.044	0.371	0.076	0.112	0.055	0.050
I	0.444	0.893	0.066	0.180	0.078	0.022	0.024	0.016
1.69 R	0.335	0.348	0.065	0.363	0.086	0.120	0.059	0.050
I	0.448	0.845	0.083	0.176	0.097	0.028	0.035	0.022
1.96 R	0.322	0.387	0.068	0.355	0.081	0.124	0.060	0.052
I	0.424	0.796	0.100	0.169	0.114	0.032	0.045	0.024
2.25 R	0.329	0.418	0.101	0.350	0.064	0.125	0.048	0.059
I	0.401	0.747	0.090	0.162	0.104	0.032	0.047	0.024

matrices as discussed by Nesbet⁶ and Nesbet and Oberoi.¹¹ For each of the energies and angular momenta considered here, we have obtained variational estimates using four (and sometimes five) methods: Kohn, inverse Kohn, optimized minimum norm (OMN), inverse OMN, and for some cases optimized anomaly free (OAF). These methods are described in the references just cited. Results which showed apparent anomalies were discarded; the rest were averaged. The spread of the results gives some indication of the error in the calculation. However, this is apparently quite small as far as the elastic total cross section is concerned, since the elastic scattering is dominated by states $L=0, S=1$ and $L=1, S=1$. In these cases, there is generally excellent agreement between the results of the different variational methods employed.

Calculations of elastic scattering in the energy range of interest that are of accuracy comparable to the present work have been performed only for the states $L=0, S=0$, and $S=1$ by McDonald and Nuttall¹² using an extrapolation from complex energies and for $S=0, L=0$, and $L=1$ by Rescigno and Reinhardt¹³ who used techniques based on the Fredholm determinant. However, the latter authors present their results in graphical form; consequently, the only detailed comparison of amplitudes possible is with the work of McDonald and Nuttall. This is shown in Table I.

The method used by McDonald and Nuttall is quite different from that employed here. The rather good agreement between the results shown in Table I increases confidence in both methods. It is not possible to assess the significance of the small differences between the amplitudes at the present time; however, it should be noted that in the low-energy region below the $n=2$ threshold, the present work yields phase shifts for $L=0, S=0$ that are smaller than the essentially exact results of Schwartz¹⁴ by about (1-2)%, while for $L=0, S=1$ the disagreement with Schwartz amounts to only 0.1%.

The elastic-scattering amplitudes as obtained from the pseudostate calculation are listed in Table II for values of the total angular momentum

$0 \leq L \leq 3$ and for all of the energies considered here. These amplitudes are normalized so that, below the inelastic threshold at $k^2 = 0.75$, they become simple $\exp(i\delta_{L,S}) \sin \delta_{L,S}$, where $\delta_{L,S}$ is the phase shift for angular momentum L and spin S . Each element f listed in Table II is related to the corresponding element T of the usual transition matrix T by $f = -\frac{1}{2}iT$.

III. EXTENSION TO $L < 4$

The contribution from values of L in the range $4 \leq L \leq 99$ was obtained using the "extended polarization" method in a manner similar to that applied¹⁵ in a calculation of the elastic scattering of electrons by helium. It is assumed that the scattering for large L is dominated by the interaction components of longest range r^{-4} and r^{-6} . The coefficients of these terms can be obtained exactly: that of r^{-4} is simply $-\alpha_d$ (the dipole polarizability), while the next term is determined by the difference between the coefficient β of r^{-6} in the leading nonadiabatic correction to the polarization interaction ("distortion potential," see Callaway *et al.*⁷), and the quadrupole polarizability α_q . In order to avoid unphysical singularities, it is convenient to define a smooth effective potential

$$V = -\alpha_d r^2 / (r^2 + b^2)^3, \quad (1)$$

where

$$b^2 = (\beta - \alpha_q) / 3\alpha_d = \frac{69}{54}. \quad (2)$$

The potential has been constructed to vanish at the origin, in accordance with the reference cited immediately above; however, use of the more common Buckingham form will not produce large differences in the phase shifts for the angular momenta and energies considered here. For partial waves of $L=4$ or 5, the phase shifts were found by solving the scattering equation of the extended polarization method⁷ containing the potential (1) in addition to the ordinary Coulomb and exchange interactions; for $L > 6$ it is sufficient to use a simple expression derived from the partial-wave Born approximation:

$$\tan \delta_L = \frac{\pi \alpha_d k^2}{(2L+3)(2L+1)(2L-1)} \left(1 - \frac{9b^2 k^2}{(2L+5)(2L-3)} + \frac{60b^4 k^4}{(2L+7)(2L+5)(2L-3)(2L-5)} + \dots \right). \quad (3)$$

Differential cross sections have been computed using the scattering amplitude and phase shifts calculated as described above.

IV. EXPERIMENTAL APPROACH

The elastic cross sections have been measured with an apparatus and method which have been used

previously for the measurement of electron-atomic-hydrogen inelastic $n=2$ excitation cross sections¹⁶ from 50–680 eV and of elastic cross sections¹ from 0.5–8.7 eV. The paper by Williams and Willis¹⁶ contains complete details of the apparatus and experimental procedures, the method of absolute cross-section calibration, and the determination of experimental errors. The apparatus is based on the crossed-electron modulated-atom beam technique. The incident beam is energy-analyzed by a 127° cylindrical electrostatic analyzer with input and output planar electron optical lenses. The beam characteristics at the interaction region have been shown to be a size of 1.2 mm (height) by 3 mm (width, along the neutral beam axis), beam angle of 0.01 rad, pencil angle of 0.01 rad, beam current of 1×10^{-7} A at an energy spread of 0.060 eV, and an energy of 20 eV, for example. The scattered electrons are analyzed by an identical 127° cylindrical electrostatic analyzer with an input acceptance angle of 0.03 rad which enabled the analyzer to see all of the interaction volume for all scattering angles. For the present elastic-scattering measurements, this analyzer was operated in a high-transmission (95%) mode with an energy pass band of 0.095 eV.

The output of the scattered-electron analyzer was collected by a channel electron multiplier, fed into a standard ORTEC 50- Ω current pulse amplifier and discriminator and then fed into either (i) scalars gated synchronously with the neutral beam chopper or (ii) a similarly gated

multichannel analyzer. The apparatus was operated automatically to permit data-taking times of about 20 h for each data point to obtain statistical errors of 2% with 98% confidence limits.

The hydrogen-atom beam originated from a tungsten oven source in which molecular hydrogen was generally 96% dissociated at low source pressures of less than 0.3 mm Hg. The dissociation fraction and the beam purity were checked by a quadrupole mass filter situated after the interaction region. The unscattered primary-electron beam was collected in a zonal Faraday cup, which contained several entrance apertures of different diameters to collect 10^{-2} and 10^{-4} of the total beam current which passed into the Faraday cup proper. By rotation of this collector through the primary beam it was possible to establish the spatial characteristics of the beam. The beam overlap integral has been studied in detail¹⁶ for all incident-electron beam energies of this paper and for scattering angles from 10°–140°.

The elastic angular distributions at each energy have been made absolute by measuring at 60° the ratio of the cross section at each energy to that at an energy of 8.70 eV, for which the absolute value of $0.727\pi a_0^2 \text{ sr}^{-1}$ had been determined previously¹ by (a) a phase-shift analysis of the elastic scattering of electrons from helium around the 19.35-eV ²S resonance, (b) measurement of relative densities for helium and hydrogen beams, and (c) molecular-hydrogen dissociation fractions.

Estimated errors associated with the measure-

TABLE III. Absolute differential elastic cross sections for the scattering of electrons from atomic hydrogen. Units are $a_0^2 \text{ sr}^{-1}$. The numbers in parenthesis are the total errors (with a 90% confidence limit) in the last significant digits and include both systematic and random errors; for example, at 20 eV and 60°, the cross section value is $(0.794 \pm 0.083) a_0^2 \text{ sr}^{-1}$.

Angle (degrees) \ Energy (eV) k (a_0^{-1})	0.94	1.1	1.2	1.3	1.4	1.5
10	7.23(78)	5.32(57)
15	6.19	3.51(37)
20	5.11	4.49(47)	3.93(44)	3.41(39)	3.13(37)	2.74(28)
25	4.31(49)	2.25(21)
30	3.69(38)	3.12(34)	2.64(29)	2.40(27)	1.98(23)	1.60(18)
40	2.70(25)	2.21(27)	2.04(21)	1.59(18)	1.32(15)	1.15(12)
50	2.05(18)	1.57(17)	1.22(14)	0.990(107)	0.779(84)	0.641(65)
60	1.50(15)	1.03(11)	0.794(83)	0.611(59)	0.544(57)	0.461(52)
70	1.20(11)	0.779(81)	0.561(56)	0.489(50)	0.356(38)	0.316(28)
80	0.98(9)	0.618(63)	0.403(41)	0.336(35)	0.264(27)	0.221(21)
90	0.830(71)	0.526(54)	0.383(41)	0.273(29)	0.206(22)	0.162(17)
100	0.744(77)	0.445(46)	0.317(33)	0.235(26)	0.177(19)	0.131(11)
110	0.691(61)	0.387(42)	0.288(32)	0.212(27)	0.163(19)	0.128(14)
120	0.689(69)	0.398(41)	0.243(27)	0.202(28)	0.147(18)	0.105(10)
130	0.700(70)	0.362(38)	0.216(26)	0.178(21)	0.132(15)	0.098(10)
140	0.711(71)	0.356(38)	0.208(27)	0.167(22)	0.119(15)	0.091(9)

ments are discussed in detail and listed in a previous paper.¹⁶ Each estimation has been made at least at a "good confidence level" which is comparable with the 70% confidence level applied to statistical uncertainties. If separate error determinations are judged to have a possible correlation with each other they are added linearly. These sums are then added in quadrature with the uncorrelated errors to obtain a total experimental error of $\pm 17\%$ with a confidence level of 70%. The actual errors for each cross-section value are listed in Table III.

V. EXPERIMENTAL RESULTS AND COMPARISON WITH THEORY

The experimental cross sections are given in numerical form in Table III and in graphical form in Figs. 1 and 2 along with the theoretical results. Numerical values for the theoretical cross sections are given in Table IV.

In Fig. 1, the present experimental data are not in agreement with the measurements of Teubner *et al.*² at angles less than 50° . Their values have been taken from the graph in their publication.² A linear cross-section scale is used to emphasize this disagreement. Both sets of measurements claim a relative error of $\pm 2\%$ between any two points over the angular distribution, whereas the difference in the angular dependence between the two sets of data is seen to be much greater than 2%. A similar disagreement occurred between their 9.4-eV angular distributions and those of Williams¹ at 8.7 eV. Support for the latter data is claimed by their agreement within the experimental error of $\pm 6\%$ with the "exact" variationally calculated cross sections at 8.7 eV, which were computed from the phase shifts of Schwartz¹⁴ for the *s* wave, of Armstead¹⁷ for the *p* wave, and of Gailitis¹⁸ for the *d* wave and the effective range expansion for the next seven higher phase shifts. This excellent agreement at 8.7 eV between the exact variational values and the values measured by Williams¹ with the same apparatus provides support also for the magnitude of the present experimental data. The angular distributions (with an error of $\pm 2\%$) of Teubner *et al.* were normalized from measurements of the ratio (with an error of 8%) of the elastically scattered atomic-to-molecular signals, assuming the molecular elastic-scattering cross-section value at 60° of Trajmar *et al.*¹⁹ (with an error of 35%). In turn, Trajmar *et al.* had measured molecular angular differential cross sections from 10° – 80° , and then extrapolated the data to 0° and 180° in order to obtain a total cross-section value which, in turn, was normalized to the absolute measurement by

Golden *et al.*²⁰ (with an error of $\pm 3\%$). The sum of all these errors gives a total possible error of $\pm 48\%$ to the data of Teubner *et al.* It is this error which is shown in Fig. 1 by a dashed error bar which limits further deductions from their data.

The present theoretical values are in agreement well within the total experimental error of $\pm 17\%$ with the present experimental values. Similarly, good agreement between experiment and theory is obtained for the early close-coupling predictions of Burke *et al.*^{21,22} except for angles smaller than about 20° . At these angles, the three-state (1*s*, 2*s*, 2*p*) predictions are lower than the six-state (1*s* to 3*d*) predictions, both of which show a quadratic small-angle dependence as opposed to the

TABLE IV. Theoretical differential cross sections for the scattering of electrons from atomic hydrogen in units of $a_0^2 \text{sr}^{-1}$. The total elastic cross section σ_e is given in units of πa_0^2 .

Angle (deg)	0.90	1.21	1.44	1.69	1.96	2.25
0	9.404	9.171	9.039	8.908	8.601	8.154
3	8.693	8.345	8.135	7.932	7.569	7.072
6	7.909	7.454	7.173	6.907	6.500	5.970
9	7.199	6.662	6.330	6.021	5.590	5.052
12	6.555	5.960	5.593	5.255	4.817	4.287
15	5.972	5.337	4.947	4.593	4.157	3.647
18	5.443	4.782	4.380	4.018	3.594	3.112
24	4.529	3.847	3.440	3.083	2.696	2.282
30	3.772	3.098	2.706	2.370	2.028	1.687
36	3.146	2.497	2.129	1.823	1.529	1.257
42	2.629	2.016	1.679	1.406	1.157	0.946
48	2.205	1.633	1.329	1.090	0.882	0.720
54	1.859	1.331	1.060	0.852	0.680	0.558
60	1.578	1.095	0.856	0.674	0.532	0.440
66	1.353	0.912	0.701	0.543	0.424	0.353
72	1.173	0.771	0.586	0.445	0.345	0.289
78	1.031	0.664	0.501	0.374	0.288	0.240
84	0.921	0.583	0.438	0.323	0.246	0.202
90	0.838	0.524	0.393	0.287	0.217	0.174
96	0.777	0.481	0.360	0.263	0.197	0.153
102	0.735	0.451	0.338	0.248	0.185	0.139
108	0.710	0.431	0.322	0.239	0.177	0.130
114	0.700	0.419	0.311	0.232	0.173	0.124
120	0.701	0.411	0.302	0.226	0.168	0.120
126	0.711	0.406	0.295	0.219	0.162	0.114
132	0.729	0.402	0.288	0.209	0.154	0.1077
138	0.751	0.399	0.280	0.197	0.143	0.0993
144	0.775	0.395	0.271	0.183	0.130	0.0896
150	0.800	0.390	0.261	0.169	0.116	0.0796
156	0.822	0.386	0.252	0.156	0.1037	0.0702
162	0.841	0.381	0.243	0.144	0.0930	0.0622
168	0.856	0.378	0.237	0.136	0.0849	0.0563
174	0.865	0.375	0.233	0.130	0.0799	0.0527
180	0.868	0.375	0.231	0.129	0.0783	0.0515
σ_e	5.796	4.158	3.414	2.829	2.346	1.946

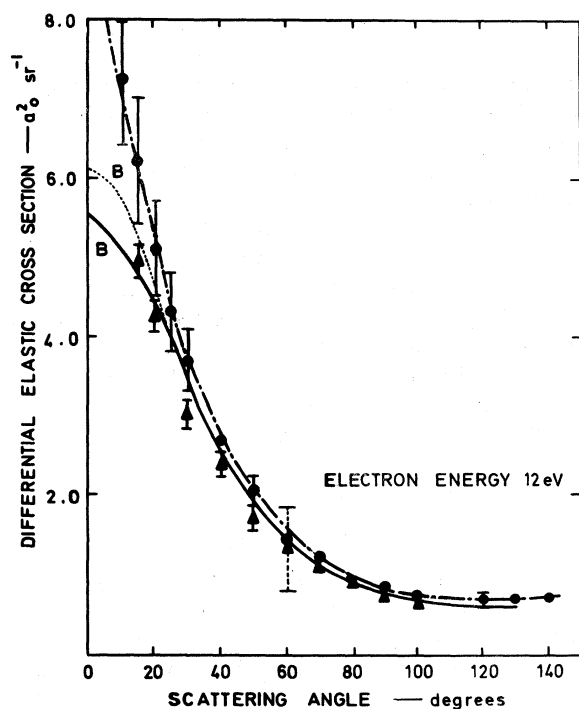


FIG. 1. Differential elastic cross section for the scattering of 12.0-eV ($k=0.94a_0^{-1}$) electrons from atomic hydrogen. Present experimental values (\bullet); present theoretical values (---) ($k=0.95a_0^{-1}$); the experimental values of Teubner *et al.* (\blacktriangle); three-state close-coupling values (Burke *et al.*, Ref. 21) (—B); and six-state close-coupling values (Burke *et al.*, Ref. 22) (---B).

relatively linear behavior of the present predicted and measured values. The plotted close-coupling values in Fig. 1 have been taken from the paper of Teubner *et al.*, whose values appear to be based on the published reactance matrices of Burke *et al.*²¹ at $k^2=0.81$ (11 eV) for the three-state approximation and of Burke *et al.*²² at $k^2=0.9$ (12.2 eV) for the six-state approximation.

Figure 2 shows the agreement between our theoretical and experimental data on a logarithmic cross-section scale to emphasize the large-angle behavior. At energies of 16.51, 20.01, 23.12 and 26.59 eV (corresponding approximately to electron momenta k values of 1.1, 1.2, 1.3 and $1.4a_0^{-1}$, respectively) a linear scale would show the same good agreement between theory and experiment as was shown in Fig. 1 at 12.10 eV. At angles larger than about 100° , the theoretical values are slightly higher than the experimental values. At 30 eV, there is good agreement between the present theoretical and experimental values. The 30-eV data of Lloyd *et al.*³ agree within the combined experimental errors with the present data,

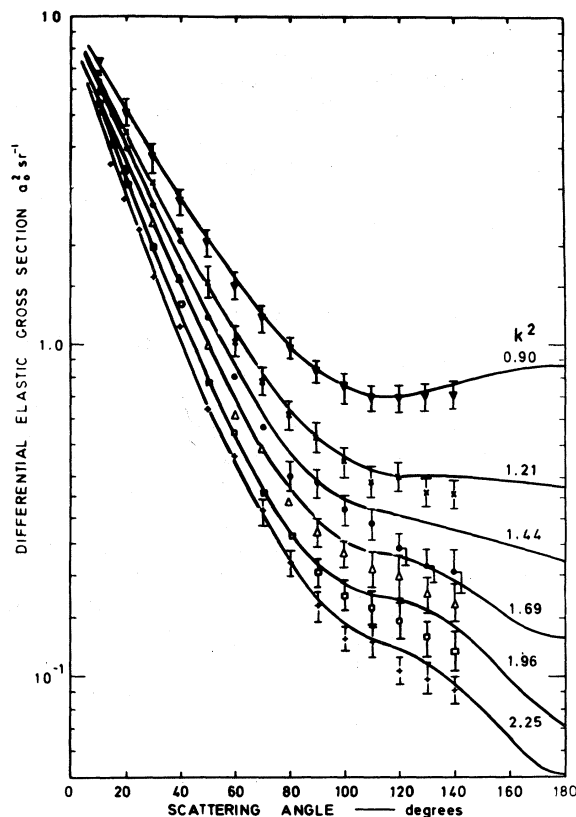


FIG. 2. Differential elastic cross section for the scattering of electrons of energies of 12.0 eV ($k^2=0.90a_0^{-2}$) (∇); of 16.51 eV ($k^2=1.21a_0^{-2}$) ($\times\times\times$); 20.01 eV ($k^2=1.44a_0^{-2}$) (\bullet); 23.12 eV ($k^2=1.69a_0^{-2}$) (Δ); 26.59 eV ($k^2=1.96a_0^{-2}$) (\square); and 30.0 eV ($k^2=2.25a_0^{-2}$) ($+$) from atomic hydrogen. The theoretical values were calculated for the above values of k^2 and are shown by full lines, while the experimental values were measured at the above energies.

while the 20-eV data of Teubner *et al.*² are up to a factor of 1.5 lower than the present data.

The source and significance of the remaining discrepancies between theory and experiment are not known at present. Neglect of partial waves for $L \geq 100$ would not be expected to have any influence on the cross section at large angles. One possible source of error in the theory is the neglect of the effects of inelastic scattering on the scattering amplitude for $L \geq 4$. In order to investigate whether this is the cause of the discrepancy, calculations have been made in which the effect of the neglected inelastic channels is included by the unitarized Born approximation with exchange, while the $1s-1s$ element of the R matrix is obtained from the extended polarization approximation. The elements of the transition matrix obtained in this way are in fairly good agreement

with, but slightly smaller than, those obtained from published three-state close-coupling results.²¹ Unlike three-state close coupling, the full atomic polarizability is included in the 1s-1s element. The changes in the calculated differential cross sections with respect to those shown here are quite minor and do not remove the disagreement at large angles.

Recently, Fon, Kingston, and Burke have presented results of a calculation of the differential cross section for elastic scattering at selected energies from 12–680 eV using a close-coupling method containing the 1s state and a $2\bar{p}$ pseudostate.²³ The calculations are carried to sufficiently high values of L with this basis to ensure convergence of the partial-wave sum. Their results appear to be in good agreement with the present theoretical calculations in the portion of the energy range where there is overlap. In particular, at 20 eV and angles greater than 100° , the results of Fon, Kingston, and Burke are also slightly larger than the experimental values given here. At 12 and 30 eV, the present experimental results agree rather closely with their calculations, as well as with our own calculations.

In conclusion, the first detailed experimental study has been made of the inelastic differential cross section over the intermediate energy region from 12–30 eV. This energy region presents no more experimental difficulties than exist at lower or higher energies; however, this is the region where channel coupling effects present most difficulties for theoretical studies of the scattering problem. It has been shown that the present pseudostate calculations can predict differential cross-section values over this energy range which are in agreement with our measured values within the present experimental error of $\pm 17\%$, except for angles greater than 120° for energies from 20–26 eV. It is not clear whether the disagreement over that small angular and energy range originates in experiment or in theory.

ACKNOWLEDGMENTS

One of us (J. C.) was an S. R. C. Senior Visiting Fellow during the period of this work and is also indebted to Dr. L. A. Morgan for providing the extended polarization phase shifts for $L = 4$ and 5. The experimental work was supported by a grant from the Science Research Council.

*Permanent address: Department of Physics and Astronomy, Louisiana State University, Baton Rouge, La. 70803.

¹J. F. Williams, *J. Phys. B* **8**, 1683 (1975).

²P. J. O. Teubner, C. R. Lloyd, and E. Weigold, *Phys. Rev. A* **9**, 2552 (1974).

³G. R. Lloyd, P. J. O. Teubner, and B. R. Lewis, *Phys. Rev. A* **10**, 175 (1974).

⁴J. Callaway and J. W. Wooten, *Phys. Rev. A* **9**, 1924 (1974).

⁵J. Callaway and J. W. Wooten, *Phys. Rev. A* **11**, 1118 (1975).

⁶R. K. Nesbet, *Phys. Rev.* **179**, 60 (1969).

⁷J. Callaway, R. W. LaBahn, R. T. Pu, and W. M. Duxler, *Phys. Rev.* **168**, 12 (1968).

⁸G. J. Seiler, R. S. Oberoi, and J. Callaway, *Phys. Rev. A* **3**, 2006 (1971).

⁹P. G. Burke and T. G. Webb, *J. Phys. B* **3**, L131 (1970).

¹⁰P. G. Burke and J. F. B. Mitchell, *J. Phys. B* **6**, 320 (1973).

¹¹R. K. Nesbet and R. S. Oberoi, *Phys. Rev. A* **6**, 1855 (1972).

¹²F. A. McDonald and J. Nuttall, *Phys. Rev. A* **4**, 1821 (1971).

¹³T. N. Rescigno and W. P. Reinhardt, *Phys. Rev. A* **10**, 158 (1974).

¹⁴C. Schwartz, *Phys. Rev.* **124**, 1468 (1961).

¹⁵R. W. LaBahn and J. Callaway, *Phys. Rev.* **180**, 91 (1969).

¹⁶J. F. Williams and B. A. Willis, *J. Phys. B* **8**, 1641 (1975).

¹⁷R. L. Armstead, *Phys. Rev.* **171**, 91 (1968).

¹⁸M. K. Gaillitis, *Zh. Eksp. Teor. Fiz.* **47**, 160 (1964) [*Sov. Phys.—JETP* **20**, 107 (1965)].

¹⁹S. Trajmar, D. G. Truhlar, and J. K. Rice, *J. Chem. Phys.* **52**, 4502 (1970).

²⁰D. E. Golden, H. W. Bandel, and J. A. Salerno, *Phys. Rev.* **146**, 40 (1966).

²¹P. G. Burke, H. M. Schey, and K. Smith, *Phys. Rev.* **129**, 1258 (1963).

²²P. G. Burke, S. Ormonde, and W. Whitaker, *Proc. Phys. Soc. Lond.* **92**, 319 (1967).

²³W. C. Fon, A. E. Kingston, and P. G. Burke, Abstracts in the *Proceedings of the Ninth International Conference on Electronic and Atomic Collisions*, edited by J. S. Risley and R. Geballe (University of Washington Press, 1975), p. 669.